

InAs/GaAs single-electron quantum dot qubit

Shu-Shen Li,^{a)} Jian-Bai Xia, Jin-Long Liu, Fu-Hua Yang, Zhi-Chuan Niu, Song-Lin Feng, and Hou-Zhi Zheng

National Laboratory for Superlattices and Microstructures, Institute of Semiconductors, Chinese Academy of Sciences, P.O. Box 912, Beijing 100083, Peoples Republic of China

(Received 19 April 2001; accepted for publication 12 September 2001)

The time evolution of the quantum mechanical state of an electron is calculated in the framework of the effective-mass envelope function theory for an InAs/GaAs quantum dot. The results indicate that the superposition state electron density oscillates in the quantum dot, with a period on the order of femtoseconds. The interaction energy E_{ij} between two electrons located in different quantum dots is calculated for one electron in the i th pure quantum state and another in the j th pure quantum state. We find that E_{11} , E_{12} , E_{22} , and E_{ij} decreases as the distance between the two quantum dots increases. We present a parameter-phase diagram which defines the parameter region for the use of an InAs/GaAs quantum dot as a two-level quantum system in quantum computation. A static electric field is found to efficiently prolong the decoherence time. Our results should be useful for designing the solid-state implementation of quantum computing. © 2001 American Institute of Physics. [DOI: 10.1063/1.1416855]

I. INTRODUCTION

Quantum computing combines computer science with quantum mechanics and is a fast growing research field.¹ A quantum computer was introduced by Benioff in 1980.² In 1982, Feynman pointed out that in order to simulate a quantum system, the computer has to operate quantum mechanically,³ i.e., one needs a quantum computer (QC). A proposal for practical implementation of a QC was presented in 1993. The elementary unit of quantum information in a QC is the quantum bit (qubit). A single qubit can be envisaged as a two-state system such as a spin-half particle or a two-level atom. The potential power of a QC is based on the ability of quantum systems to be in a superposition of its basic states. In order to perform quantum computations, one should have the following basic conditions: (i) a two-level system ($|0\rangle$ and $|1\rangle$) as a qubit; (ii) the ability to prepare the qubit in a given state, say $|0\rangle$; (iii) the capability of measuring each qubit; (iv) the ability to perform basic gate operations such as a conditional logic gate (the control-not gate); and (v) a sufficiently long decoherence time. It is very important for a QC to be well isolated from any environmental interaction which would destroy the superposition of states. Furthermore, one has to use quantum error correction, which has been devised recently.

Several schemes, like trapped ions,⁴ quantum optical systems,⁵ nuclear and electron spins,^{6–8} and superconductor Josephson junctions^{9–12} have been proposed for realizing quantum computation. However, in order to show its superiority over the most advanced classical computers, quantum computers need to be composed of at least thousands of qubits to be feasible. To this end, it is clear that quantum computation with a significant number of qubits would be more realizable in solids,¹³ especially by invoking semiconductor

nanostructures or quantum dots (QDs).¹⁴ The ground state ($|0\rangle$) and the first excited state ($|1\rangle$) of an electron in a QD may be employed as a two-level quantum system. An electromagnetic pulse can be applied to drive an electron from $|0\rangle$ to $|1\rangle$ or to the superposition state of $|0\rangle$ and $|1\rangle$. To perform a quantum-controlled “not” manipulation, one may simply apply a static electric field by placing a gate near the QD.

However, before quantum computation can be realized using QDs, two main obstacles must be overcome. First, high-quality, regularly spaced, uniform semiconductor QDs must be fabricated. Today, using the Stranski–Krastanov method, the fabrication of self-assembled InAs/GaAs QDs of high quality may not be very difficult by various types of modern epitaxy technologies like molecular-beam epitaxy, but the growth of regularly spaced, uniform, self-assembled QDs remains a severe challenge for such a technology. The second key issue is how to prolong the decoherence time in semiconductor QDs when there exist innumerable degrees of freedom which dephase the systems very fast.

Bertoni *et al.* studied the oscillation of the electron density between two coupled quantum wires, which can be used to realize the universal set of quantum logic gates.¹⁵ In this article, we shall study the dephasing rate, time evolution of the quantum state of the electron in an InAs/GaAs QD, and the interaction of the two electrons located in different QDs. Our calculated results should be useful for designing the solid-state implementation of quantum computing.

This article is arranged as follows. In Sec. II we give a theoretical model for calculating the electronic states. In Sec. III, we show the numerical results. Finally, we give the conclusions in Sec. IV.

II. THEORETICAL MODEL

To study an InAs/GaAs self-assembled QD in an electric field, we choose the growth direction (100) as the z

^{a)}Electronic mail: sslee@red.semi.ac.cn

direction of our coordinate system, and assume the InAs self-assembled QD to be a cylinder. The height of the QD in the z direction is L . In the parallel direction, the radius of the QD is R . According to Burt and Foreman's effective mass envelope function theory,^{16,17} by neglecting the second- and higher-order terms, the effective Hamiltonian of electrons in the presence of an electric field \mathbf{F} along the z axis can be written as follows

$$H_e = \mathbf{P} \frac{1}{2m^*(\mathbf{r})} \mathbf{P} + V(\mathbf{r}) - eFz, \quad (1)$$

where \mathbf{P} is the electron momentum operator,

$$m^*(\mathbf{r}) = \begin{cases} m_1^* & \text{for } |z| < L/2 \text{ and } x^2 + y^2 < R^2, \\ m_2^* & \text{elsewhere,} \end{cases} \quad (2)$$

$$V_e(\mathbf{r}) = \begin{cases} 0 & \text{for } |z| < L/2 \text{ and } x^2 + y^2 < R^2, \\ V_{e0} & \text{elsewhere,} \end{cases} \quad (3)$$

and m_1^* and m_2^* are the electron effective masses in the InAs and GaAs media, respectively. The electron envelope function equation is written as

$$H_e \Psi_e = E_e \Psi_e, \quad (4)$$

which can be solved for the eigenvalues and eigenfunctions of the system by expanding Ψ_e in terms of normalized plane-wave states and diagonalizing the resultant matrix. We assume that the electron wave functions have the following forms:

$$\Psi_e(\mathbf{r}) = \frac{1}{\sqrt{L_x L_y L_z}} \times \sum_{nml} C_{nml} e^{i[(k_x + nK_x)x + (k_y + mK_y)y + (k_z + lK_z)z]}, \quad (5)$$

with $K_x = 2\pi/L_x$, $K_y = 2\pi/L_y$, and $K_z = 2\pi/L_z$. Here, L_x , L_y , and L_z are the normalized lengths along the x , y , and z directions, respectively. For a cylindrical QD, we take $L_x = L_y$, and $n, m, l = 0, \pm 1, \pm 2, \dots$. The matrix elements of Hamiltonian Eq. (1) in the basis function given by Eq. (5) can be written as

$$\left(\frac{\hbar^2}{2m_2^*} \delta + \frac{\hbar^2}{2m_1^*} S_i S_j \right) (k_{nx} k'_{nx} + k_{my} k'_{my} + k_{lz} k'_{lz}) + (\delta - S_i S_j) V_{e0} + F_{l,l'}, \quad (6)$$

where $1/m_{12}^* = 1/m_1^* - 1/m_2^*$, $k_{nx} = (k_x + nK_x)$, $k'_{nx} = (k_x + n'K_x)$, $k_{my} = (k_y + mK_y)$, $k'_{my} = (k_y + m'K_y)$, $k_{lz} = (k_z + lK_z)$, and $k'_{lz} = (k_z + l'K_z)$. The δ function is given by

$$\delta = \begin{cases} 1 & \text{for } n=n' \text{ and } m=m' \text{ and } l=l', \\ 0 & \text{for } n \neq n' \text{ or } m \neq m' \text{ or } l \neq l', \end{cases} \quad (7)$$

and

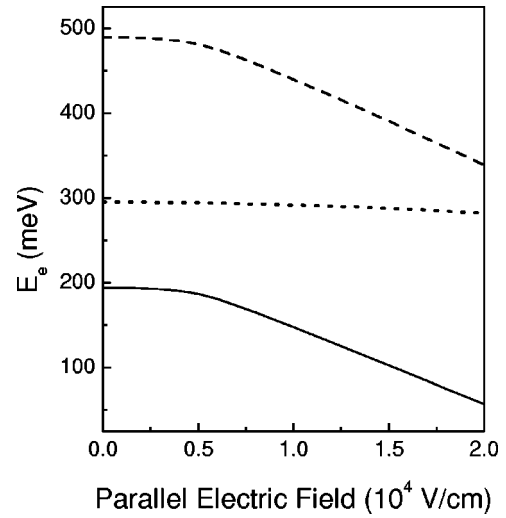


FIG. 1. Energy spacing between $|0\rangle$ and $|1\rangle$ (solid line) and energy levels of $|0\rangle$ (dotted line) and $|1\rangle$ (dashed line) vs parallel electric field. The radius and height of the QD are taken as 5 nm.

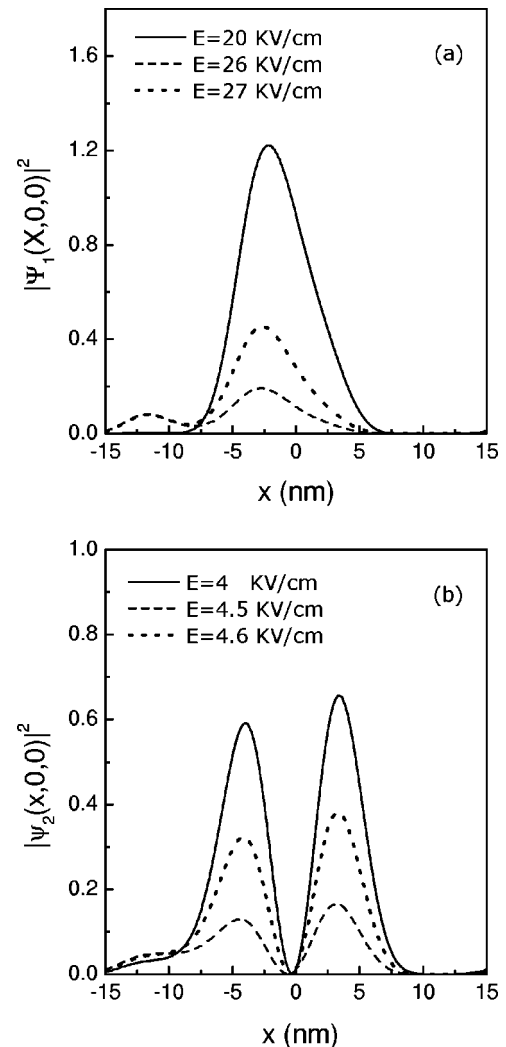


FIG. 2. Wave function distributions of $|0\rangle$ (a) and $|1\rangle$ (b) vs the parallel coordinate x for different values of the electric field along the x -direction. The radius and height of the QD are taken as 5 nm.

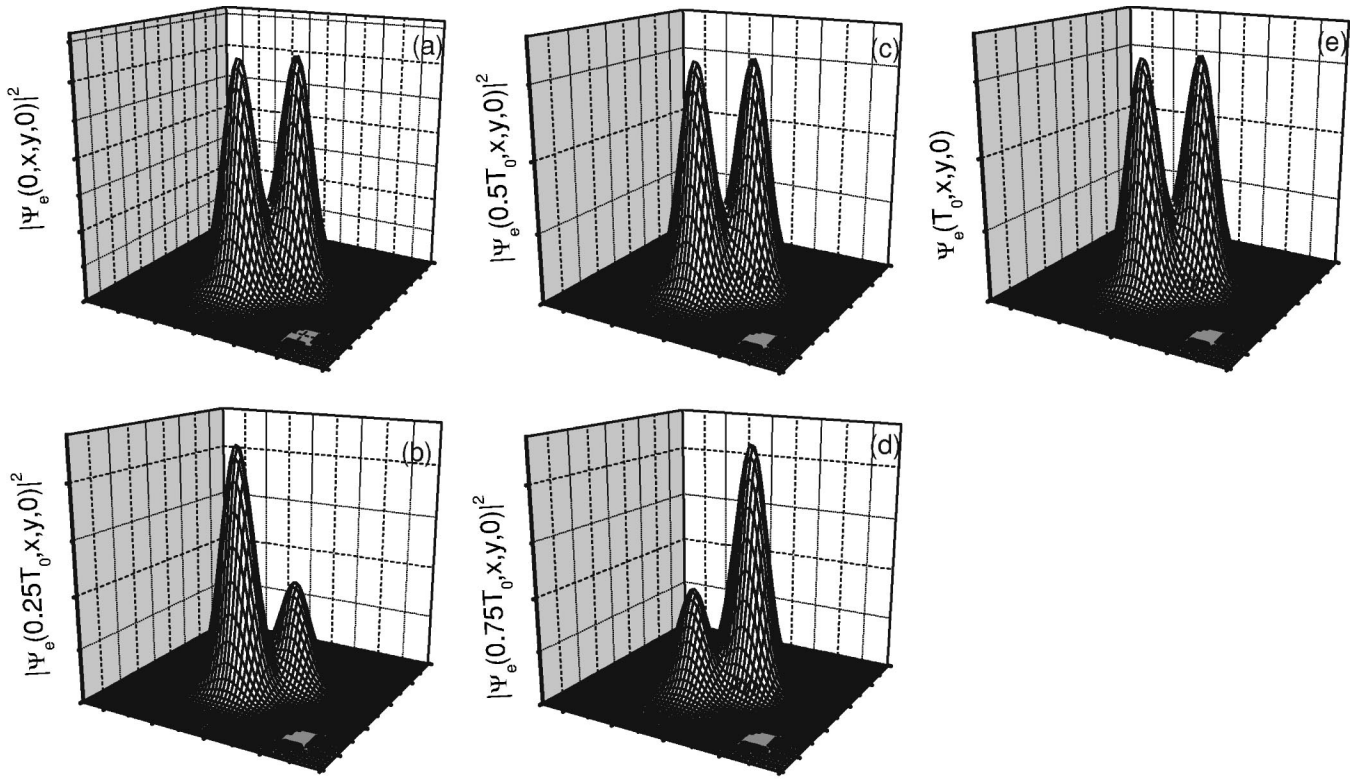


FIG. 3. Time evolution of the electron superposition of $|0\rangle$ and $|1\rangle$. The radius and height of the QD are taken to be 5 and 4 nm, respectively. Time t in (a), (b), (c), (d), and (e) are 0, 0.25, 0.5, 0.75, and $1 T_0$, respectively.

$$S_i = \begin{cases} \frac{L}{L_z} & \text{for } l=l', \\ \frac{\sin\left[\pi(l-l')\frac{L}{L_z}\right]}{\pi(l-l')} & \text{for } l \neq l', \end{cases} \quad (8)$$

$$S_j = \begin{cases} \frac{\pi R^2}{L_x^2} & \text{for } n=n' \text{ and } m=m', \\ \frac{R}{\lambda L_x} J_1(\lambda K_x R) & \text{for } n \neq n' \text{ or } m \neq m', \end{cases} \quad (9)$$

$$F_{l,l'} = \begin{cases} 0 & \text{for } l=l', \\ ieF \frac{(-1)^{l-l'} L_z}{2\pi(l-l')} & \text{for } l \neq l'. \end{cases} \quad (10)$$

In Eq. (9) $\lambda = \sqrt{(n-n')^2 + (m-m')^2}$, and $J_1(x)$ is the first-order Bessel function of x . We can then calculate the electron states in the vertical electric field from Eq. (6). If electric field \mathbf{F} is in the plane, we can obtain similar results.

The issue of dephasing in QDs has already been addressed in the literature.^{15,18-23} Impurities and thermal vibration (phonons) can reduce the lifetime to $\sim 10^{-9}$ s or even worse, but, in principle, their effects can be minimized by a more precise fabrication technology, by cooling the crystal, and by choosing the state and the physical parameters properly.¹⁴ It must be pointed out that the decoherence time decreases if the temperature decreases, but, when we reach the $E_2 - E_1$ K T limit, the decoherence time does not decrease

any more. In the present model, we assume a large energy difference between $|0\rangle$ and $|1\rangle$, so we can neglect the acoustic and optical phonon scattering and only take into account the decoherence coming from the vacuum fluctuation. Under the dipole approximation, based on the Fermi Golden Rule,²⁴ the spontaneous emission rate can be written in the following form:

$$\tau^{-1} = \frac{e^2 \Delta E}{3 \pi \epsilon_0 \hbar^2 m_0^2 C^3} \sqrt{\frac{\epsilon}{\epsilon_0}} |\langle 0 | \mathbf{r} | 1 \rangle|^2, \quad (11)$$

where C is the speed of light in vacuum, ϵ (ϵ_0) is the material (vacuum) dielectric constant, ΔE is the energy level spacing between $|0\rangle$ and $|1\rangle$, and τ is the decoherence time.

The time evolution of the quantum state of the electron can be written as

$$\Psi_e(t, \mathbf{r}) = \frac{1}{\sqrt{2}} \Psi_e^1(\mathbf{r}) e^{-itE_1/\hbar} + \frac{1}{\sqrt{2}} \Psi_e^2(\mathbf{r}) e^{-itE_2/\hbar}. \quad (12)$$

The Coulomb interaction energy between two electrons located in different QDs can be calculated using

$$E_{ij} = \int \frac{|\Psi^i(\mathbf{r}_1)|^2 |\Psi^j(\mathbf{r}_2)|^2}{4 \pi \epsilon |\mathbf{r}_1 - \mathbf{r}_2|} d\mathbf{r}_1 d\mathbf{r}_2, \quad (13)$$

where $|\mathbf{r}_1 - \mathbf{r}_2| = \sqrt{(x_1 - x_2)^2 + (y_1 - y_2)^2 + (z_1 - z_2)^2}$, and ϵ is the material dielectric constant.

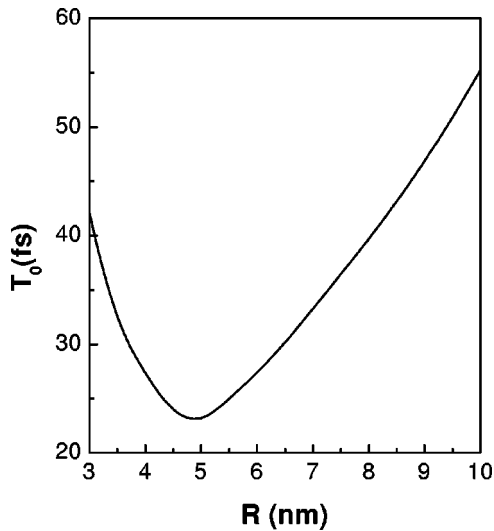


FIG. 4. Period of oscillation $T_0 = h/(E_2 - E_1)$ vs QD radius. The height of the QD is taken to be 5 nm.

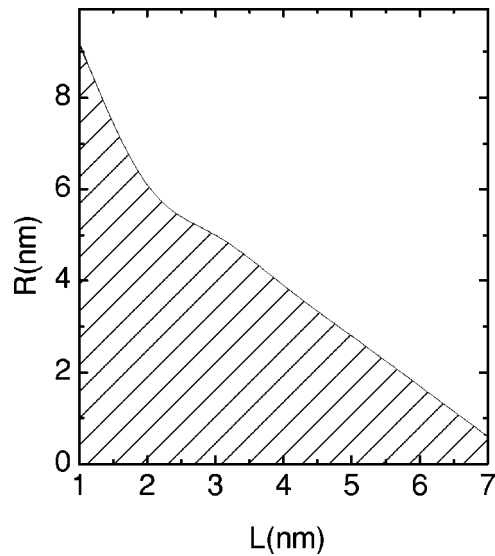


FIG. 6. Shape of the parameter-phase diagram of one InAs/GaAs QD used as a qubit. The gray region indicates that the QD cannot be used as a qubit.

III. RESULTS AND DISCUSSION

We take the effective masses of InAs and GaAs to be 0.023 and 0.067 m_0 , and the band gaps to be 0.418 and 1.518 eV, respectively.²⁵ The conduction-band offset is assumed to be 70% of the band-gap difference.²⁶ The material dielectric constant ϵ is equal to 12.25 ϵ_0 .

Figure 1 shows the energy spacing ΔE between $|0\rangle$ and $|1\rangle$ (solid line) and the energy levels of $|0\rangle$ (dotted line) and $|1\rangle$ (dashed line) as a function of the parallel electric field. The radius and height of the QD are taken to be 5 nm. It turns out that the energy of $|0\rangle$ does not depend on the electric field sensitively. However as long as the electric field is larger than 5 kV/cm, the energy of $|1\rangle$ and ΔE decrease substantially with increasing electric field.

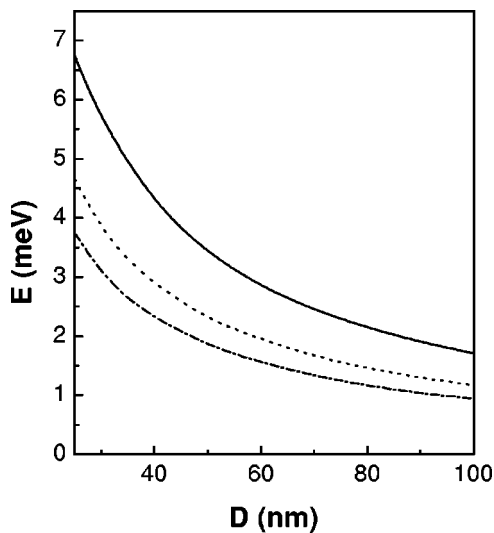


FIG. 5. Interaction energy between two electrons located in different QDs as a function of the distance between the centers of two QDs. The solid, dotted, and dashed lines indicate the interaction energies between $|0\rangle$ and $|0\rangle$, $|0\rangle$ and $|1\rangle$, and $|1\rangle$ and $|1\rangle$, respectively. The radius and height of the QDs are taken to be 5 and 4 nm, respectively.

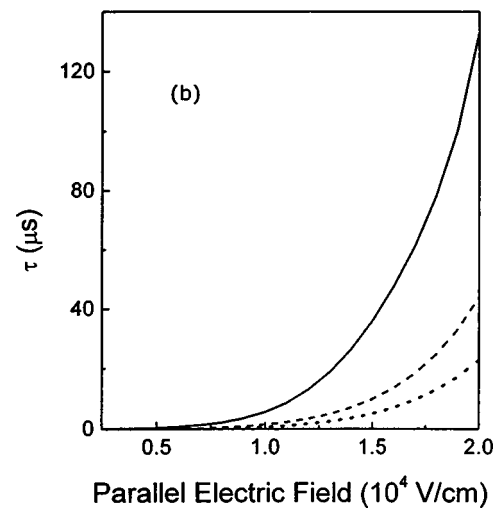
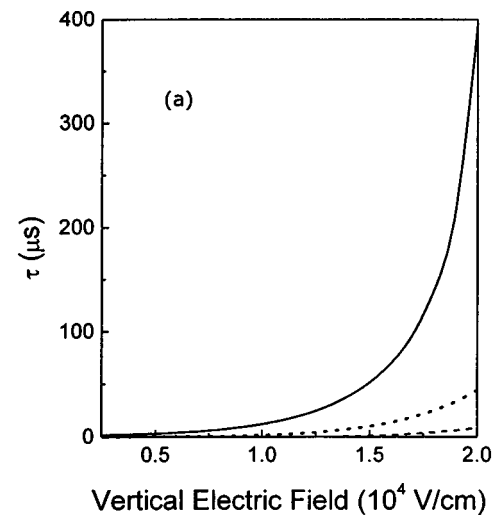


FIG. 7. Decoherence time vs vertical static electric field (a) and parallel static electric field (b) for different QD heights: 4 nm (solid lines), 5 nm (dotted lines), and 6 nm (dashed lines). Radius of the QD is taken as 5 nm.

Figure 2 plots the wave-function distributions of the $|0\rangle$ state (a) and $|1\rangle$ state (b) as a function of coordinate x in different x -direction electric fields. The radius and height of the QD are also 5 nm. Figure 2 clearly shows that the static electric field induces a change of the electron charge distribution in the QD which is opposite for $|0\rangle$ and $|1\rangle$. The induced dipole moment points in the same direction as the electric field for $|0\rangle$, but is in the opposite direction for $|1\rangle$.

Figure 3 shows the time evolution of the electron density $|\Psi_e(t, x, y, 0)|^2$ when the electron is in the superposition state: $1/\sqrt{2}(|0\rangle + |1\rangle)$. The radius and height of the QD are taken to be 5 and 4 nm, respectively. We find that the electron oscillates in the QD, with a period $T_0 = h/(E_2 - E_1) \approx 23$ fs for the above material and shape parameters. The time t in Figs. 3(a), 3(b), 3(c), 3(d), and 3(e) are 0, 0.25, 0.5, 0.75, and 1 T_0 , respectively.

Figure 4 plots the period of oscillation $T_0 = h/(E_2 - E_1)$ as a function of the radius of the QD. The height of the QD is taken to be 4 nm. From Fig. 4 we find that (i) the oscillation period decreases as the radius of the QD decreases because the energy difference $(E_2 - E_1)$ increases; (ii) there is a minimum in the oscillating period curve; and (iii) if the radius is smaller than the critical value, the period of oscillation increases as the radius decreases. The reason is that there is only one confined quantum state (the ground state $|0\rangle$) in the QD when the radius is smaller than the critical value. The excited quantum states are continuous states located above the barrier. The energies of the continuous states are close to the top of the barrier and do not depend sensitively on the radius of the QD.

The interaction energy between electrons located in different QDs is a very important parameter in designing quantum gates. Figure 5 shows the interaction energies between two electrons located in different QDs as a function of the distance between the centers of the two QDs. The solid, dotted, and dashed lines indicate the interaction energies between $|0\rangle$ and $|0\rangle$, $|0\rangle$ and $|1\rangle$, and $|1\rangle$ and $|1\rangle$, respectively. The interaction energies decrease as the distance increases.

A QD that can be used in quantum computation must consist of at least two binding states. Figure 6 shows the parameter-phase diagram of one InAs/GaAs QD. The gray region in Fig. 6 indicates that only one binding state resides in the QD. In contrast, there are at least two binding states in the white region so that the QD may be used as a qubit.

Figures 7(a) and 7(b) show the decoherence times as a function of the vertical and parallel static electric fields, respectively, for the same radius (5 nm) and three different heights of 4 nm (solid lines), 5 nm (dotted lines), and 6 nm (dashed lines). From Fig. 7 we find that the decoherence time does not depend on the electric field sensitively until the strength of the electric field is lower than 5 kV/cm. The decoherence time then increases very fast as the electric field goes beyond 5 kV/cm. The decoherence time may reach an order of magnitude of milliseconds under a 20 kV/cm static electric field for the QD with 5 nm radius and 4 nm height.

IV. SUMMARY

We have studied the time evolution and dephasing rate of the electron superposition state of the ground and first

excited states for a model InAs quantum dot embedded in GaAs. The energy levels and wave functions of the ground and first excited states of an electron in a static electric field have been calculated in the framework of the effective-mass envelope function theory. The calculated results indicate that the density of electrons in the superposition state oscillates in the QD. The oscillation period is on the order of femtoseconds. The interaction energy E_{ij} between two electrons is calculated for one electron in the i th quantum state and another in the j th quantum state. We find that $E_{11} > E_{12} > E_{22}$, and E_{ij} decreases as the distance between two QDs increases. We present the parameter-phase diagram which defines the parameter region for the use of an InAs/GaAs QD as a two-level quantum system in quantum computation. A static electric field is found to efficiently prolong the decoherence time, which may even reach milliseconds when the external static electric field exceeds 20 kV/cm, if vacuum fluctuation is taken as the only source of decoherence. Our results should be useful for designing the solid-state implementation of quantum computing.

ACKNOWLEDGMENTS

This work was partly supported by the National Natural Science Foundation of China and the Hundred Talents Program of Chinese Academy of Sciences.

- ¹C. H. Bennett and D. P. DiVincenzo, *Nature (London)* **404**, 247 (2000).
- ²P. Benioff, *J. Stat. Phys.* **22**, 563 (1980).
- ³R. Feynman, *Int. J. Theor. Phys.* **21**, 467 (1982).
- ⁴J. I. Cirac and P. Zoller, *Phys. Rev. Lett.* **74**, 4091 (1995).
- ⁵Q. A. Turchette, C. J. Hood, W. Lange, H. Mabuchi, and H. J. Kimble, *Phys. Rev. Lett.* **75**, 4710 (1995).
- ⁶N. A. Gershenfeld and I. L. Chuang, *Science* **275**, 350 (1997).
- ⁷B. E. Kane, *Nature (London)* **393**, 133 (1998).
- ⁸D. Loss and D. P. DiVincenzo, *Phys. Rev. A* **57**, 120 (1998).
- ⁹D. V. Averin, *Solid State Commun.* **105**, 659 (1998).
- ¹⁰Y. Makhlin, G. Schon, and A. Shnirman, *Nature (London)* **398**, 305 (1999).
- ¹¹L. B. Ioffe, V. B. Geshkenbein, M. V. Feigelman, A. L. Fauchere, and G. Blatter, *Nature (London)* **398**, 679 (1999).
- ¹²Y. Nakamura, Yu. A. Pashkin, and J. S. Tsai, *Nature (London)* **398**, 786 (1999).
- ¹³G. P. Berman, G. D. Doolen, and V. I. Tsifrinovich, *Superlattices Microstruct.* **27**, 89 (2000).
- ¹⁴A. Barenco, D. Deutsch, A. Ekert, and R. Jozsa, *Phys. Rev. Lett.* **74**, 4083 (1995).
- ¹⁵A. Bertoni, P. Bordone, R. Brunetti, C. Jacoboni, and S. Reggiani, *Phys. Rev. Lett.* **84**, 5912 (2000).
- ¹⁶M. G. Burt, *J. Phys.: Condens. Matter* **4**, 6651 (1992).
- ¹⁷B. A. Foreman, *Phys. Rev. B* **52**, 12 241 (1995).
- ¹⁸J. P. Bird, K. Ishibashi, D. K. Ferry, Y. Ochiai, Y. Anoyagi, and T. Sugano, *Phys. Rev. B* **51**, 18 037 (1995).
- ¹⁹R. M. Clarke, I. H. Chan, C. M. Marcus, C. I. Duruöz, J. S. Harris, Jr., K. Campman, and A. C. Gossard, *Phys. Rev. B* **52**, 2656 (1995).
- ²⁰A. G. Huibers, J. A. Folk, S. R. Patel, C. M. Marcus, C. I. Duruöz, and J. S. Harris, Jr., *Phys. Rev. Lett.* **83**, 5090 (1999).
- ²¹A. G. Huibers, M. Switkes, C. M. Marcus, K. Campman, and A. C. Gossard, *Phys. Rev. Lett.* **81**, 200 (1998).
- ²²A. Yu. Smirnov, N. J. M. Horing, and L. G. Mouroukh, *J. Appl. Phys.* **87**, 4525 (2000).
- ²³G. Tóth and C. S. Lent, *Phys. Rev. A* **63**, 052315 (2001).
- ²⁴L. D. Landau and E. M. Lifshitz, *Quantum Mechanics (Nonrelativistic Theory)* (Pergamon, London, U. K., 1987).
- ²⁵*Numerical Data and Functional Relationships in Science and Technology*, Landolt-Bornstein, New Series (Springer, Berlin, 1982), Vol. 17a.
- ²⁶P. D. Wang, N. N. Ledentsov, C. M. Sotomayer Torres, P. S. Kop'ev, and V. M. Ustinov, *Appl. Phys. Lett.* **64**, 1526 (1994).